Title: Lack of RNase HI affects virulence in *Salmonella enterica*

Authors: Julia Jiménez-Espadafor[1,2], Miriam Ortiz-Padilla[1†], Diego A. Pedraza-Delgado[1†], Joaquín Bernal-Bayard[1], Francisco Ramos-Morales[1]* and Roberto Balbontín[1]*.

Affiliations:

[1]Departamento de Genética, Facultad de Biología, Universidad de Sevilla. Avda. Reina Mercedes, 6. 41012 Sevilla. Spain.

[2]Department of Biology, Science4Life, Utretch University. Padualaan 8, Utretch. 3584 CH. The Netherlands.

[†]these authors contributed equally.

*Correspondence to: rbalbontin@us.es and framos@us.es.

Abstract:

Bacterial virulence and antibiotic resistance are interconnected global threats that can synergize, multiplying their adverse effects on health and economy. Two proposed strategies to address this dual challenge are non-biocidal inhibition of virulence traits (anti-virulence strategy) and manipulation of eco-evolutionary dynamics in bacterial populations to hamper dissemination of antibiotic resistance (anti-resistance strategy). These strategies require to identify factors involved in bacterial gene expression, fitness and evolution. R-loops strongly influence these traits, as well as fitness of bacteria carrying antibiotic resistance mutation, making the enzyme responsible for R-loop degradation, the RNase HI, a promising target for anti-resistance approaches. Interestingly, the extensive involvement of R-loops in transcription initiation and termination could also make RNase HI a potential target for anti-virulence strategies. Here we explored this possibility by investigating the effects of RNase HI deficiency on traits associated with pathogenicity in the human pathogen *Salmonella enterica* serovar Typhimurium. We found that lack of RNase HI alters expression of virulence genes at population and single-cell levels, and both *ex vivo* and during infection of mammalian cells. Moreover, we showed that RNase HI depletion causes defects in phenotypes associated with virulence, such as motility, biofilm formation, and resistance to low pH. Coherently, we observed that the absence of RNase HI reduces *Salmonella*'s ability to survive within macrophages. Altogether, our results demonstrate the influence of R-loops on bacterial virulence, suggesting that RNase HI could serve as a target for anti-virulence strategies. This provides a theoretical framework for the development of dual anti-resistance and anti-virulence interventions based on RNase HI targeting.

INTRODUCTION

The world is currently entering a so-called post-antibiotic era[1]. With a reduced palette of effective antibiotics, bacterial pathogens may cause an enormous health and economic burden worldwide[2]. For instance, mortality associated to antibiotic-resistant infections is estimated to exceed that of cancer by 2050[3], and was almost 5 millions in 2019[4] . Moreover, there is growing evidence base linking antibiotic resistance and climate change[5], increasing the scopes of these global challenges. The capacity of bacteria to cause disease is a critical aspect of the antibiotic resistance crisis. Indeed, antibiotic resistance and bacterial virulence can be conceived as two sides of the same coin, as bacterial pathogens represent a smaller threat if treated with effective antibiotics, and antibiotic resistant bacteria pose a lesser challenge if not able to develop pathogenesis. In addition, antibiotic resistance and bacterial virulence can influence one another, multiplying their combined detrimental effects on global health and economy[6]. Thus, there is an imperative need to develop novel strategies to tackle bacterial pathogens and antibiotic resistance, also addressing their reciprocal influence[1].

Salmonella enterica is a Gram-negative bacterial species that encompasses over 2500 serovars[7], able to infect a broad range of hosts, causing from gastroenteritis to systemic infection, depending on the serovar and the host[8]. Many *S. enterica* pathogenic functions are encoded by virulence genes, some clustered in horizontally acquired genomic regions known as *Salmonella* pathogenicity islands (SPIs)[9–12], which encode secretion systems able to inject into the host cells bacterial proteins known as effectors[13]. These effectors promote invasion of host cells by bacteria and interfere with host functions in order to facilitate pathogenesis[14]. Two of the most relevant and well-studied SPIs are SPI-1 and SPI-2, which encode two distinct Type III Secretion Systems (T3SS) and are involved in invasion of the intestinal epithelium and proliferation within mammalian cells[15], respectively. *Salmonellae* are responsible for a large mortality and morbidity in human populations, as well as a vast economic loss

due to infections of farming animals[16,17]. Thus, novel therapeutical interventions against infections caused by *S. enterica*, particularly by antibiotic-resistant strains, are urgently needed.

Two promising approaches recently proposed to tackle the double threat of bacterial virulence and antibiotic resistance are anti-virulence therapy (non-biocidal suppression of pathogenic traits)[18] and anti-resistance strategy (selection against resistant bacteria by exploitation of eco-evolutionary dynamics in bacterial populations)[19]. A key aspect for the development of either strategy is identifying specific targets involved in bacterial pathogenesis or evolution. Interestingly, bacterial cells contain molecular structures, called R-loops, which influence both regulation of gene expression and bacterial evolution[20–23]. Thus, mechanisms involved in R-loop biology could potentially serve as targets for both anti-virulence and anti-resistance therapies.

R-loops are RNA-DNA hybrids formed during transcription, upon the invasion of the DNA template strand by the nascent RNA[24], which are essential for bacterial gene expression, fitness and evolution[20–23]. R-loops participate in key physiological processes, such as transcription initiation and termination, regulation of gene expression, DNA repair, etc. However, if elevated, R-loops can cause transcription stalling, blocks to replication fork progression, inhibition of DNA repair, replication-transcription conflicts and DNA breaks[25]. Thus, R-loops need to be maintained within an optimal range to remain harmless for the cell[26–28]. RNase HI, whose function is conserved along the phylogenetic tree, is one of the key factors involved in R-loop homeostasis, as it specifically degrades RNA in R-loops[29,30].

We recently showed that depleting RNase HI function (either genetically or chemically) strongly reduces the fitness of *Escherichia coli* carrying mutations conferring resistance to rifampicin and/or streptomycin[31]. Indeed, lack of RNase HI leads to extinction of resistant clones when competing

against susceptible bacteria even at high initial frequency of resistance, abolishing compensatory evolution, both *ex vivo* and in the mammalian gut[31]. Interestingly, a subsequent study ratified the validity of depleting RNase HI as an antimycobacterial treatment[32]. Thus, RNase HI is a promising target for anti-resistance approaches.

The involvement of R-loops in transcription[33,34], and therefore in gene expression, makes possible that R-loop imbalance caused by lack of RNase HI affects expression of virulence genes, altering the capacity of bacterial pathogens to timely and efficiently develop the expression program that leads to pathogenesis. Indeed, other ribonucleases have been shown to play a central role in the control of bacterial virulence[35,36], including regulation of SPIs in *Salmonella enterica*[37,38].

Thus, RNase HI function, which is susceptible to chemical inhibition[31], could potentially constitute a convergent target for both anti-resistance and anti-virulence approaches that remained unexplored to date. Here we investigated the involvement of R-loops in *S. enterica* virulence, and found that expression of genes associated with pathogenesis are significantly altered in the absence of RNase HI, both at population and single-cell levels. We also demonstrate that phenotypes related to virulence, such as biofilm formation, motility and survival in low pH, are reduced in a strain lacking RNase HI. Finally, we showed that lack of RNase HI negatively affects the capacity of *S. enterica* to survive within mammalian cells. Altogether, our results indicate that RNase HI could also be a promising target for anti-virulence strategies, thus constituting a novel dual target for the aforementioned approaches and anti-resistance treatments.

RESULTS

Salmonella *lacking RNase HI shows a mild fitness defect*

We first constructed a *Salmonella* strain carrying a scarless in frame deletion in the *rnhA* gene, which encodes RNase HI. The deletion was designed in a way that does not affect a promoter of the downstream gene *dnaQ*, which is located within the coding sequence of *rnhA*[39], and rendered a shorter version of the RNase HI lacking amino acids 44-153, which encompass its catalytic region[30]. We then measured the fitness of the *ΔrnhA* mutant strain and wild-type bacteria by running growth curves and competitions in Lysogeny Broth (LB)[40]. Although growth curves of both strains are almost indistinguishable (Figure 1A), competitions show a 9% fitness defect of the *ΔrnhA* mutant with respect to the wild type (Figure 1B).

Lack of RNase HI alters expression of genes associated with virulence

In order to test if R-loop imbalance affects expression of genes important for virulence, we took advantage of a collection of luciferase reporter fusions available in the laboratory[41], and we selected a set of 15 genes involved in processes relevant to virulence, such as SPIs, iron uptake, quorum sensing or Type VI Secretion Systems (Table 1). We measured the expression levels of these genes in wild type and *ΔrnhA* strains three different conditions: i) under standard laboratory conditions (LB with shaking), ii) under conditions of induction of SPI-1 (static cultures in LB with 0.3M of NaCl)[42], and iii) in a medium that mimics the intracellular millieu of mammalian cells (Low Phosphate and Magnesium medium, LPM) and induces SPI-2[43]. As Figure 2 shows, expression of most genes is significantly altered in the *ΔrnhA* mutant in at least one of the conditions tested (Figure 2A), causing in most cases a negative effect (Figure 2B-D). However, upregulation can be observed in certain genes and conditions; for instance, genes encoding SPI-2 effectors *sseK3*, *ssaV*, and the enterobactin non-ribosomal peptide synthetase *entF* in conditions of SPI-2 induction, and the synthase of the quorum molecule autoinducer-2 *luxS* in LB and conditions of SPI-1 induction (Figure 2A).

The absence of RNase HI affects expression of SPI-1 at the single-cell level

Expression of the SPI-1 is not homegeneous across the entire population of *S. enterica*. Instead, its expression shows bistability; that is, the SPI-1 is expresssed only in a subset of the total population, whereas another fraction of the population does not express it[44]. Since lack of RNase HI affects the expression of a SPI-1 gene (*iagB*), we next tested if RNAse HI depletion influences expression of SPI-1 at the single-cell level. We constructed wild-type and *ΔrnhA* strains carrying: i) a copy of the gene encoding the superfolder green fluorescent protein (*sfGFP* hereafter) under the control of the promoter of the SPI-1 gene *sicA*, inserted in the pseudogene locus *malYX*, and ii) a copy of the gene encoding the *mCherry* red fluorescent protein under the control of a constitutive promoter, inserted in the pseudogene STM14_2013. These strains allowed us to distinguish viable bacteria (those expressing *mCherry*) from compromised or dead cells, and measure by flow cytometry percentages of viable bacteria expressing the SPI-1 (green fluorescent bacteria) in each genetic background (Figure 3A). Interestingly, we observed that lack of RNase HI significantly affects the percentage of bacteria that expresses SPI-1 both in rich (Figure 3B, top panel) and minimal medium (Figure 3B, bottom panel), demonstrating that R-loop imbalance influences bistability in the expression of SPI-1.

The results described above confirm that lack of RNase HI alters expression of genes encoding proteins directly involved in virulence, such as T3SS effectors, but also influences genes coding for proteins involved in mechanisms relevant for bacterial physiology that can influence pathogenesis, such as synthesis of enterobactin, signal transduction, and synthesis and processing of the quorum sensing molecule autoinducer-2[45–47]. Particularly, some of these regulatory circuits can influence phenotypes previously connected with bacterial pathogenesis. For instance, quorum sensing has been shown to affect both biofilm formation, bacterial motility and virulence[48,49]. Conversely, SPI-1 has been

reported to modulate *Salmonella* motility[50]. This intrincate cross-regulation opens the possibility that RNase HI depletion pleiotropically affects multiple phenotypes associated with virulence, such as biofilm formation and motility.

175 *RNase HI depletion causes defects in biofilm formation*

We thus first measured the ability to form biofilms of the *ΔrnhA* mutant, using the well-established colony morphology assay in LB without salt[51], wild-type bacteria as negative control, and a mutant lacking the master regulator of biofilm formation CsgD (*ΔcsgD*) as positive control. Figure 4A shows
180 that the strain lacking RNase HI is able to form wrinkly structures similar to those of the wild type, and different from the smooth colonies formed by the *ΔcsgD* positive control. However, colonies of *ΔrnhA* are unable to expand radially as wild-type colonies do, presenting a somewhat intermediate phenotype, not as smooth as the *ΔcsgD* control but not as structured and expanded as wild-type bacteria. In order to quantify these differences, we compared the same genotypes using the crystal violet assay[52,53]. This
185 allowed us to ratify that the mutant lacking RNase HI is not able to form biofilms as wild-type bacteria, but still forms better biofilms than the *ΔcsgD* control (Figure 4B). Using negative and positive controls as references, the ability to form biofilms of the *ΔrnhA* mutant is approximately 35% of the wild type (Figure 4C).

190 *Lack of RNase HI negatively influences bacterial motility*

Another phenotype linked to virulence and connected with some of the genes whose expression is altered by RNase HI depletion is motility. We next used the bacterial motility assay[54] to analyze motility of the wild-type (as negative control), bacteria lacking RNase HI and a non-flagellated
195 *ΔfliGHI* mutant[55] as positive control, and found that the mutant lacking RNase HI is less motile than the

wild type, but not completely non-motile, as the *ΔfliGHI* mutant (Figure 5A). With respect to positive and negative control, the *ΔrnhA* mutants shows around 60% the motility of the wild type (Figure 5B).

Expression of SPI-2 is altered in the ΔrnhA mutant during infection of mammalian epithelial cells

In order to test if the influence of R-loops on expression of virulence genes also occurs *in vivo*, we then constructed wild-type and *ΔrnhA* strains carrying the P_{sicA}-*sfGFP* reporter fusion of the SPI-1 described above and a second P_{ssaB}-*mCherry* reporter fusion in which the *mCherry* is under the control of the promoter of the SPI-2 gene *ssaB*, inserted in the pseudogene locus *STM14_2013*. These double reporter strains allow to simultaneously measure expression of both SPI-1 and SPI-2 by flow cytometry using wild-type and *ΔrnhA* strains carrying constitutively expressed *sfGFP* or *mCherry* as controls. We infected human HeLa human epithelial cells with these wild-type and *ΔrnhA* strains carrying the double reporter for SPI-1 and SPI-2 or the constitutively expressed *sfGFP* and *mCherry*, and analyzed the number of bacterial cells expressing each island along the infection. Strains constitutively expressing each fluorescence allowed us: i) to monitor progression of the infection in each genetic background (Figure 6A) and ii) to set up a threshold distinguishing fluorescent from non-fluorescent bacterial cells, and therefore which ones can be considered to have SPI-1 and/or SPI-2 activated. We found that, albeit at 30 minutes after infection the wild-type and the mutant lacking RNase HI show very similar expression patterns, at 24 hours the *ΔrnhA* shows a significantly greater percentage of cells expressing SPI-2 than wild-type bacteria (Figure 6B).

Lack of RNase HI negatively affects Salmonella's ability to proliferate within mammalian macrophages

The fact that lack of RNase HI alters expression of SPI-1, SPI-2, and other genes associated with virulence, together with its effects on phenotypes relevant for pathogenesis, such as motiliy and biofilm

formation, may cause the *ΔrnhA* mutant to be defective in virulence. To test this, we next performed competitions of either the wild type, the *ΔrnhA* mutant or a double mutant where SPI-1 and SPI-2 are deleted (*ΔSPI-1 ΔSPI-2* hereafter)[56] against a reference wild-type strain labeled with a constitutively expressed *lacZ* during infection of RAW264.7 murine macrophages[57]. As Figure 7 shows, the capacity of the mutant lackin RNase HI is severely impaired with respect to the wild type, showing proliferation similar to that of the *ΔSPI-1 ΔSPI-2* positive control.

DISCUSSION

The advent of the post-antibiotic era poses the greatest challenge to modern medicine in human history. Numerous medical interventions require efficient antibiotics (e.g. surgery, dental care, treatment of traumatic injuries, etc.), and multiple medical conditions enhance susceptibility to bacterial pathogens (e. g. cancer, AIDS, etc.), making functional antibiotics a necessity to protect the population affected by these conditions[58,59]. Thus, novel strategies to treat bacterial infections and/or prevent the development and dissemination of antibiotic resistances are urgently needed. Anti-resistance and anti-virulence strategies have been proposed as innovative approaches to tackle the increasing threat of antibiotic resistant pathogens[18,19]. We recently reported that the enzyme responsible for degradation of R-loops, the RNase HI, is involved in maintenance of fitness in bacteria carrying antibiotic resistance mutations[31], being thus a promising candidate as target for anti-resistance approaches. Moreover, the role of R-loops in transcription made plausible that depletion of RNase HI function could affect expression of genes relevant for virulence and therefore cause reduced pathogenicity. We tested this hypothesis by analyzing the effects of lacking RNase HI on phenotypes linked to *Salmonella*'s virulence. We found that, despite not causing a great fitness defect (Figure 1), lack of RNase HI significantly affects expression of multiple genes related to virulence, including genes involved in signal transduction, metal uptake, quorum sensing and genes in SPI-1 and SPI-2 (Figure 2). These

effects on expression of virulence genes also occurs at single-cell level (Figure 3), and during infection of mammalian cells (Figure 6). Moreover, several phenotypes relevant for pathogenicity, such as biofilm formation (Figure 4), and motility (Figure 5), are also affected by RNase HI depletion. Indeed, proliferation within mammalian macrophages is as reduced in a strain lacking RNase HI as in a mutant where SPI-1 and SPI-2 have been deleted (Figure 7). This suggest that altered expression of genes associated with virulence caused by the excess of R-loops in the absence of RNase HI renders *Salmonella* unable to properly develop the transcriptional program required for efficient pathogenesis. For instance, reduced motility decreases bacterial ability to swim towards mammalian cells[59], and defective biofilms affects attachment to mammalian tissues[60]. In addition, excess of R-loops has consequences for bacterial physiology that are particularly disadvantageous during infection. For instance, preliminary results indicate that the mutant lacking RNase HI shows reduced survival at low pH (Figure S1), which is a condition characteristic of the intracellular millieu. Moreover, misregulation of virulence genes affects both invasion and proliferation, likely due to incoordination of both the assembly of the secretion machinery and translocation of effector proteins[61], but perhaps also via triggering a stronger immune response in the host. If the latter is true, this would open the possibility of using RNase HI mutants as live vaccines[62].

In the onset of a post-antibiotics era, where one of the biggest achievements of modern medicine is under siege, novel approaches to tackle bacterial infections and to reduce antibiotic resistance are desperately needed. In summary, our results demonstrated that R-loop imbalance pleiitropically affects multiple virulence traits, making it a suitable target for anti-virulence strategies. Importantly, as previous results revealed the potential of RNase HI as a target for anti-resistance interventions[31,32], RNase HI could become a dual target for both anti-virulence and anti-resistance strategies, which would represent a promising intervention against one of the most pressing challenges of global health.

MATERIALS AND METHODS

Bacterial strains, media, and growth conditions

All strains in this study (Table S1) are *Salmonella enterica* subspecie *enterica* serovar Typhimurium strain ATCC 14028s[63]. Mutant strains were constructed by Lambda-Red recombineering[64] and/or scarless DNA recombineering[65], followed by transduction to a clean genetic background mediated by P22 HT 105/1 *int201*[66]. Constitutively fluorescent strains harbor a copy of either superfolder green fluorescent protein (*sfGFP*) or mCherry fluorescent protein (*mCherry*), under the control of the P_{TetO-1} promoter, inserted in the pseudogene locus STM14_2013. These constructions were generated by Lambda-Red recombineering using preexisting constructions[67,31] as templates. Fluorescent reporter fusions were generated by one-step recombineering[68], recombineering and P22 HT 105/1 *int201* transduction. Luciferase fusions were derivatives reconstructed from fusions obtained in a previous study[41]. Cultures were grown in either lysogeny broth[40] (LB, Lennox formulation), carbon-free minimal medium (NCE)[69] broth supplemented with 0.4% glucose, LB 0.3M NaCl[42], or low phosphate, low magnesium-containing medium (LPM)[43], and incubated at 37ºC in either glass inocule tubes with or without shaking and at either 200 r.p.m in a INFORs HT Multitron Standard shaker or in round-bottom 96-well plates with shaking (700 rpm) in a Grant-bio PHMP-4 benchtop incubator. Except for motility and colony morphology assays, solid medium was LB containing 1.5% agar. Media were supplemented when necessary with antibiotics at the following concentrations: ampicillin (100 µg/mL), kanamycin (50 µg/mL), chloramphenicol (10 µg/mL), and tetracycline (20 µg/mL).

Growth curves and luciferase expression assays

Strains were streaked individually onto LB agar plates supplemented with the appropriate antibiotic, and incubated overnight at 37 °C. The next day, independent colonies from each strain were inoculated separately in LB supplemented with the appropriate antibiotic (100 µl per well) in a 96-well plate and incubated overnight at 37 °C with shaking (700 rpm). The next day, 1:20 dilutions of the overnight cultures (10µl of culture in 190µl medium) were made, and 10µl of that diluted solution was used to inoculate round-bottom 96-well plates containing 90µl of the corresponding medium. Then plates were incubated at 37 °C with double orbital shaking set as "fast" in a Biotek SYNERGY H1 benchtop microplate reader, and OD_{600}/luminiscence were measured every 30 min during 24 h.

Competitive fitness assays

The relative fitness (selection coefficient per generation) analyzed genotype was measured by competitive growth against an isogenic strain carrying a *mudJ* element (which encodes the *lacZ* gene) inserted in the gene *trg*, which was shown no to affect bacterial virulence[57], as reference. Competitor strains were first streaked out of their respective frozen vials to LB supplemented with the appropriate antibiotic, then individual colonies were inoculated separately in medium without antibiotics and incubated overnight (approximately 16 h); the next morning, the number of cells in each culture was estimated by OD_{600} and 1:1 mixtures of Lac+ and Lac- bacteria were inoculated in glass tubes and incubated at 37ºC with shaking (200 r.p.m) for 24 h. The initial and final frequencies of the strains were estimated by plating dilutions and counting Colony Forming Units (CFUs). The number of generations was estimated from that of the reference sensitive strain, and the selection coefficient was determined as described below for each independent competition. The formula used to calculate the selection coefficient was $s=\left[\ln\left(NSf/NRf\right)-\ln\left(NSi/NRi\right)\right]/\ln\left(NRf/NRi\right)$, being NRi and NRf the initial and final

number of reference bacteria, and NSi and NSf the initial and final number of the sample bacteria that is being analyzed.

Flow cytometry

Flow cytometry was performed using either a MACSQuant® Analyzer VYB flow cytometer (Miltenyi Biotec, Bergisch Gladbach, Germany) or a CytoFlex S® flow cytometer (Beckman Coulter, Brea, CA), equipped with 488 nm and 561 nm lasers used for scatter parameters and sfGFP and mCherry excitation. Regarding optical configuration for detection, sfGFP was detected using bandpass filters of 525/50 nm (MACSQuant®) or 525/40 nm (CytoFlex S®), and mCherry was detected using bandpass filters of 615/20 nm (MACSQuant®) or 610/20 nm (CytoFlex S®). To detect bacteria, the analyzers were equipped with either a photomultiplier tube (PMT) in the case of the MACSQuant® and an avalanche photodiode (APD) in the case of the CytoFlex S®. Samples were acquired using either MACSQuantify™ 2.13.3 software (MACSQuant®) or CytExpert version 2.3 software (CytoFlex S®), and analyzed using FlowJo version 10.9.0 software (Tree Star, Inc., Ashland, OR). Prior to flow cytometry measurement, bacterial cultures were diluted in filtered phosphate-buffered saline (PBS).

Colony morphology assays

Strains were streaked individually onto LB agar plates supplemented with the appropriate antibiotic, and glass tubes containing LB were inoculated with six independent colonies of each strain and incubated overnight at 37 °C. The next day, 5 µL of each culture were used to inoculate a LB agar without salt (Yeast Extract 5g/L, Tryptone 10g/L)[51] plate. Images of bacterial colonies after 7 days of incubation at 30°C were acquired using a BIO-RAD Gel Doc XR+ Molecular Imager and Image Lab version 5.1 software.

Crystal violet assays

Strains were streaked individually onto LB agar plates supplemented with the appropriate antibiotic, and glass tubes containing LB without salt (Yeast Extract 5g/L, Tryptone 10g/L)[51] were inoculated with three independent colonies of each strain and incubated overnight at 37 °C. The next day, overnight cultures were diluted 1:100 in LB without salt, six technical replicates of 100 µL from each subculture were placed in wells of a round-bottom 96-well plate to inoculate a LB without salt (Yeast Extract 5g/L, Tryptone 10g/L), and the plate was incubated at 25ºC for 48 h, without shaking. Then OD_{600} of the cultures were measured, the medium containing planctonic bacteria was removed, wells were washed three times with sterile PBS, 200 µL of methanol was added, and the plate was incubated 15 minutes at room temperature in static to fix the bacterial biofilm. After the methanol was removed, the plate was left to dry for 10 minutes at room temperature in static, 125 µL of 0.1 crystal violet was added, and the plate was incubated 15 minutes at room temperature in static to stain bacterial biofilms. Then wells were washed again three times with PBS, and the plate was left to dry for at least 2 h. Once dry, 250 µL of 33% acetic acid was added to each well, and the plate was incubated 15 minutes at room temperature in static, to dissolve the crystal violet attached to the biofilms, and then OD_{580} was measured.

Motility assays

Strains were streaked individually onto LB agar plates supplemented with the appropriate antibiotic, and glass tubes containing LB were inoculated with six independent colonies of each strain and incubated overnight at 37 °C. The next day, a sterile toothpick was soaked in each culture and used to

inoculate a motility agar plate (5 g/L NaCl, 10 g/L Tryptone, 3 g/L agar)[54]. Bacterial growth halos were compared after 14 h of incubation at 37°C.

Infection of HeLa human epithelial cells

HeLa (human epithelial; ECACC no. 93021013) cells were seeded in 24-well plates at 1.5×10^5 cells per well and incubated in DMEM supplemented with 10% fetal calf serum for 24 h at 37 °C with 5% CO2. Bacterial strains were streaked individually onto LB agar plates supplemented with the appropriate antibiotic, and glass tubes containing LB were inoculated with two independent colonies of each strain and incubated overnight at 37 °C. Then bacteria were added to the cell culture at a multiplicity of infection of 100. Cell culture was washed twice with sterile PBS 30 minutes after infection, overlaid with DMEM containing 100 µg/mL gentamicin, and incubated for another hour and a half. The culture was then washed twice with sterile PBS, covered with DMEM with gentamicin (16 µg/mL), and incubated for 22 h.

Competitive proliferation assays within RAW murine macrophages

RAW264.7 (murine macrophages; ECACC no. 91062702) cells were seeded in 24-well plates at 1.5×10^5 cells per well and incubated in DMEM supplemented with 10% fetal calf serum for 24 h at 37 °C with 5% CO2. Bacterial strains were streaked individually onto LB agar plates supplemented with the appropriate antibiotic, and glass tubes containing LB were inoculated with each strain, incubated overnight at 37 °C with shaking and added at a multiplicity of infection of 50. Cell culture was washed twice with sterile PBS 30 minutes after infection, overlaid with DMEM containing 100 µg/mL gentamicin, and incubated for another hour and a half. The culture was then washed twice with sterile PBS, covered with DMEM with gentamicin (16 µg/mL), and incubated for 22 h.

Viability spot assays at normal and low pH

For viability assays at normal and low pH, strains were first streaked out of their respective frozen vials, then individual colonies were inoculated separately in medium without antibiotics and incubated overnight (approximately 16 h); the next morning, 10^{-1}, 10^{-2}, 10^{-3}, 10^{-4}, 10^{-5}, 10^{-6} and 10^{-7} dilutions were prepared by serial dilutions in sterile PBS. Then 5 µl aliquots of these bacterial solutions (approximately 5×10^{6} to 0.5 cells) were spotted onto LB agar plates at pHs of either 6.8 or 4.9, and these plates were incubated overnight at 37 °C.

Statistical analyses

All analyses were conducted using Libreoffice Calc version 6.0.7.3 (www.libreoffice.org) software, R version 3.6.3 (www.r-project.org) software via RStudio version 1.2.1578 interface (www.rstudio.com) and GraphPad Prism version 8.0.2 (www.graphpad.com). In competitive fitness and luminiscence measurement assays, for each set of competitions, one-sample two-tailed Student's t-tests were used to determine whether the data set corresponding to each genotype is significantly different than 0. For comparing different conditions or genotypes, two-tailed unpaired Student's t-tests were used.

ACKNOWLEDGEMENTS

We are grateful to Modesto Carballo and Laura Navarro of the "Servicio de Biología" of the "Centro de Investigación, Tecnología e Innovación de la Universidad de Sevilla (CITIUS)", for their assistance with experiments performed at CITIUS facilities.

AUTHOR CONTRIBUTIONS

Conceptualization: R.B., F.R.-M., J.B.-B.; validation: R.B., J.B.-B., F.R.-M.; formal analysis: R.B., J.B.-B., F.R.-M; investigation: R.B., J.J.-E., M.O.-P, D.A.P.-D.; resources: F.R.-M., J.B.-B., R.B.; writing—original draft preparation: R.B.; writing—review and editing: R.B., J.J.-E., M.O.-P, D.A.P.-D., J.B.-B., F.R.-M.; supervision: F.R.-M., J.B.-B., R.B.; project administration: F.R.-M., J.B.-B., R.B.; funding acquisition, F.R.-M., J.B.-B., R.B. All authors have read and agreed to the published version of the manuscript.

FUNDING

This research was part of the grants PID2019-106132RB-I00 and PID2022-136863NB-I00 funded by MCIN/AEI/10.13039/501100011033 and by “ERDF a way of making Europe”, María Zambrano fellowship (MZAMBRANO-2021-20045), grant CNS2022-135955, from Plan de Recuperación, Transformación y Resiliencia «European Union-NextGenerationEU», and Emergia fellowship EMC21_00154, from Consejería de Transformación Económica, Industria, Conocimiento y Universidades from Junta de Andalucía.

REFERENCES

1. Okeke, I. N. *et al.* The scope of the antimicrobial resistance challenge. *Lancet* **403**, 2426–2438 (2024).
2. Ho, C. S. *et al.* Antimicrobial resistance: a concise update. *Lancet Microbe* **6**, 100947 (2025).
3. Tackling drug-resistant infections globally : final report and recommendations / the Review on Antimicrobial Resistance chaired by Jim O'Neill. *Wellcome Collection* https://wellcomecollection.org/works/thvwsuba/items.
4. Murray, C. J. *et al.* Global burden of bacterial antimicrobial resistance in 2019: a systematic analysis. *The Lancet* **0**, (2022).
5. van Bavel, B. *et al.* Intersections between climate change and antimicrobial resistance: a systematic scoping review. *Lancet Planet Health* **8**, e1118–e1128 (2024).
6. Cepas, V. & Soto, S. M. Relationship between Virulence and Resistance among Gram-Negative Bacteria. *Antibiotics (Basel)* **9**, E719 (2020).
7. Tindall, B. J., Grimont, P. a. D., Garrity, G. M. & Euzéby, J. P. Nomenclature and taxonomy of the genus Salmonella. *Int J Syst Evol Microbiol* **55**, 521–524 (2005).
8. Garai, P., Gnanadhas, D. P. & Chakravortty, D. Salmonella enterica serovars Typhimurium and Typhi as model organisms: revealing paradigm of host-pathogen interactions. *Virulence* **3**, 377–388 (2012).
9. Galán, J. E. & Curtiss, R. Cloning and molecular characterization of genes whose products allow Salmonella typhimurium to penetrate tissue culture cells. *Proc Natl Acad Sci U S A* **86**, 6383–6387 (1989).
10. Ochman, H., Soncini, F. C., Solomon, F. & Groisman, E. A. Identification of a pathogenicity island required for Salmonella survival in host cells. *Proc Natl Acad Sci U S A* **93**, 7800–7804 (1996).
11. Shea, J. E., Hensel, M., Gleeson, C. & Holden, D. W. Identification of a virulence locus encoding a second type III secretion system in Salmonella typhimurium. *Proc Natl Acad Sci U S A* **93**, 2593–2597 (1996).

12. Gerlach, R. G. & Hensel, M. Salmonella pathogenicity islands in host specificity, host pathogen-interactions and antibiotics resistance of Salmonella enterica. *Berl Munch Tierarztl Wochenschr* **120**, 317–327 (2007).
13. Azimi, T., Zamirnasta, M., Sani, M. A., Soltan Dallal, M. M. & Nasser, A. Molecular Mechanisms of Salmonella Effector Proteins: A Comprehensive Review. *Infect Drug Resist* **13**, 11–26 (2020).
14. Bernal-Bayard, J. & Ramos-Morales, F. Molecular Mechanisms Used by Salmonella to Evade the Immune System. *Curr Issues Mol Biol* **25**, 133–168 (2018).
15. Gerlach, R. G. & Hensel, M. Protein secretion systems and adhesins: the molecular armory of Gram-negative pathogens. *Int J Med Microbiol* **297**, 401–415 (2007).
16. Kim, S., Kang, H., Excler, J.-L., Kim, J. H. & Lee, J.-S. The Economic Burden of Non-Typhoidal Salmonella and Invasive Non-Typhoidal Salmonella Infection: A Systematic Literature Review. *Vaccines (Basel)* **12**, 758 (2024).
17. Perez-Sepulveda, B. M. & Hinton, J. C. D. Microbe Profile: Salmonella Typhimurium: the master of the art of adaptation. *Microbiology (Reading)* **171**, (2025).
18. Ogawara, H. Possible drugs for the treatment of bacterial infections in the future: anti-virulence drugs. *J Antibiot (Tokyo)* **74**, 24–41 (2021).
19. Baquero, F., Coque, T. M. & de la Cruz, F. Ecology and evolution as targets: the need for novel eco-evo drugs and strategies to fight antibiotic resistance. *Antimicrob Agents Chemother* **55**, 3649–3660 (2011).
20. Cheng, B. *et al.* RNase H overproduction allows the expression of stress-induced genes in the absence of topoisomerase I. *FEMS Microbiol Lett* **221**, 237–242 (2003).
21. Naka, K., Koga, M., Yonesaki, T. & Otsuka, Y. RNase HI stimulates the activity of RnlA toxin in Escherichia coli. *Mol Microbiol* **91**, 596–605 (2014).
22. Maduike, N. Z., Tehranchi, A. K., Wang, J. D. & Kreuzer, K. N. Replication of the Escherichia coli chromosome in RNase HI-deficient cells: multiple initiation regions and fork dynamics. *Mol Microbiol* **91**, 39–56 (2014).
23. Drolet, M. & Brochu, J. R-loop-dependent replication and genomic instability in bacteria. *DNA Repair (Amst)* **84**, 102693 (2019).

24. Thomas, M., White, R. L. & Davis, R. W. Hybridization of RNA to double-stranded DNA: formation of R-loops. *Proc Natl Acad Sci U S A* **73**, 2294–2298 (1976).
25. Sollier, J. & Cimprich, K. A. Breaking bad: R-loops and genome integrity. *Trends Cell Biol* **25**, 514–522 (2015).
26. Crossley, M. P., Bocek, M. & Cimprich, K. A. R-Loops as Cellular Regulators and Genomic Threats. *Mol Cell* **73**, 398–411 (2019).
27. García-Muse, T. & Aguilera, A. R Loops: From Physiological to Pathological Roles. *Cell* **179**, 604–618 (2019).
28. Hegazy, Y. A., Fernando, C. M. & Tran, E. J. The balancing act of R-loop biology: The good, the bad, and the ugly. *J Biol Chem* **295**, 905–913 (2020).
29. Tadokoro, T. & Kanaya, S. Ribonuclease H: molecular diversities, substrate binding domains, and catalytic mechanism of the prokaryotic enzymes. *FEBS J* **276**, 1482–1493 (2009).
30. Hyjek, M., Figiel, M. & Nowotny, M. RNases H: Structure and mechanism. *DNA Repair (Amst)* **84**, 102672 (2019).
31. Balbontín, R., Frazão, N. & Gordo, I. DNA Breaks-Mediated Fitness Cost Reveals RNase HI as a New Target for Selectively Eliminating Antibiotic-Resistant Bacteria. *Mol Biol Evol* **38**, 3220–3234 (2021).
32. Al-Zubaidi, A. *et al.* RNase HI Depletion Strongly Potentiates Cell Killing by Rifampicin in Mycobacteria. *Antimicrob Agents Chemother* **66**, e0209121 (2022).
33. Gowrishankar, J., Leela, J. K. & Anupama, K. R-loops in bacterial transcription: their causes and consequences. *Transcription* **4**, 153–157 (2013).
34. Raghunathan, N. *et al.* Genome-wide relationship between R-loop formation and antisense transcription in Escherichia coli. *Nucleic Acids Res* **46**, 3400–3411 (2018).
35. Lawal, A., Jejelowo, O., Chopra, A. K. & Rosenzweig, J. A. Ribonucleases and bacterial virulence. *Microb Biotechnol* **4**, 558–571 (2011).
36. Matos, R. G. *et al.* The Role of Ribonucleases and sRNAs in the Virulence of Foodborne Pathogens. *Front Microbiol* **8**, 910 (2017).

37. López-Garrido, J. & Casadesús, J. Regulation of Salmonella enterica pathogenicity island 1 by DNA adenine methylation. *Genetics* **184**, 637–649 (2010).
38. López-Garrido, J., Puerta-Fernández, E. & Casadesús, J. A eukaryotic-like 3' untranslated region in Salmonella enterica hilD mRNA. *Nucleic Acids Res* **42**, 5894–5906 (2014).
39. Kröger, C. *et al.* An infection-relevant transcriptomic compendium for Salmonella enterica Serovar Typhimurium. *Cell Host Microbe* **14**, 683–695 (2013).
40. Bertani, G. Studies on lysogenesis. I. The mode of phage liberation by lysogenic Escherichia coli. *J Bacteriol* **62**, 293–300 (1951).
41. de la Rosa-Altura, J. J. *et al.* Generation of Random luxCDABE Transcriptional Fusions in the Genome of Salmonella enterica. *Methods Mol Biol* **2182**, 141–151 (2021).
42. Galán, J. E. & Curtiss, R. Expression of Salmonella typhimurium genes required for invasion is regulated by changes in DNA supercoiling. *Infect Immun* **58**, 1879–1885 (1990).
43. Deiwick, J., Nikolaus, T., Erdogan, S. & Hensel, M. Environmental regulation of Salmonella pathogenicity island 2 gene expression. *Mol Microbiol* **31**, 1759–1773 (1999).
44. Hautefort, I., Proença, M. J. & Hinton, J. C. D. Single-copy green fluorescent protein gene fusions allow accurate measurement of Salmonella gene expression in vitro and during infection of mammalian cells. *Appl Environ Microbiol* **69**, 7480–7491 (2003).
45. Ratledge, C. Iron metabolism and infection. *Food Nutr Bull* **28**, S515-523 (2007).
46. de Pina, L. C. *et al.* The role of two-component regulatory systems in environmental sensing and virulence in Salmonella. *Crit Rev Microbiol* **47**, 397–434 (2021).
47. Zhang, X. *et al.* Regulatory Mechanisms between Quorum Sensing and Virulence in Salmonella. *Microorganisms* **10**, 2211 (2022).
48. Sholpan, A., Lamas, A., Cepeda, A. & Franco, C. M. Salmonella spp. quorum sensing: an overview from environmental persistence to host cell invasion. *AIMS Microbiol* **7**, 238–256 (2021).
49. Rana, K. *et al.* Association of quorum sensing and biofilm formation with Salmonella virulence: story beyond gathering and cross-talk. *Arch Microbiol* **203**, 5887–5897 (2021).
50. Saleh, D. O. *et al.* SPI-1 virulence gene expression modulates motility of Salmonella Typhimurium in a proton motive force- and adhesins-dependent manner. *PLoS Pathog* **19**, e1011451 (2023).

51. Römling, U., Sierralta, W. D., Eriksson, K. & Normark, S. Multicellular and aggregative behaviour of Salmonella typhimurium strains is controlled by mutations in the agfD promoter. *Mol Microbiol* **28**, 249–264 (1998).
52. Fletcher, M. The effects of culture concentration and age, time, and temperature on bacterial attachment to polystyrene. *Can. J. Microbiol.* **23**, 1–6 (1977).
53. O'Toole, G. A. & Kolter, R. Initiation of biofilm formation in Pseudomonas fluorescens WCS365 proceeds via multiple, convergent signalling pathways: a genetic analysis. *Mol Microbiol* **28**, 449–461 (1998).
54. Gillen, K. L. & Hughes, K. T. Negative regulatory loci coupling flagellin synthesis to flagellar assembly in Salmonella typhimurium. *J Bacteriol* **173**, 2301–2310 (1991).
55. Lockman, H. A. & Curtiss, R. Salmonella typhimurium mutants lacking flagella or motility remain virulent in BALB/c mice. *Infect Immun* **58**, 137–143 (1990).
56. Baisón-Olmo, F., Cardenal-Muñoz, E. & Ramos-Morales, F. PipB2 is a substrate of the Salmonella pathogenicity island 1-encoded type III secretion system. *Biochem Biophys Res Commun* **423**, 240–246 (2012).
57. Segura, I., Casadesús, J. & Ramos-Morales, F. Use of mixed infections to study cell invasion and intracellular proliferation of Salmonella enterica in eukaryotic cell cultures. *J Microbiol Methods* **56**, 83–91 (2004).
58. Olaru, I. D. *et al.* The association between antimicrobial resistance and HIV infection: a systematic review and meta-analysis. *Clin Microbiol Infect* **27**, 846–853 (2021).
59. Danielsen, A. S. *et al.* Clinical outcomes of antimicrobial resistance in cancer patients: a systematic review of multivariable models. *BMC Infect Dis* **23**, 247 (2023).
60. Jones, G. W., Rabert, D. K., Svinarich, D. M. & Whitfield, H. J. Association of adhesive, invasive, and virulent phenotypes of Salmonella typhimurium with autonomous 60-megadalton plasmids. *Infect Immun* **38**, 476–486 (1982).
61. Römling, U. *et al.* Occurrence and regulation of the multicellular morphotype in Salmonella serovars important in human disease. *Int J Med Microbiol* **293**, 273–285 (2003).

62. Hébrard, M., Kröger, C., Sivasankaran, S. K., Händler, K. & Hinton, J. C. D. The challenge of relating gene expression to the virulence of Salmonella enterica serovar Typhimurium. *Curr Opin Biotechnol* **22**, 200–210 (2011).

63. Bansal, G., Ghanem, M., Sears, K. T., Galen, J. E. & Tennant, S. M. Genetic engineering of Salmonella spp. for novel vaccine strategies and therapeutics. *EcoSal Plus* **12**, eesp00042023 (2024).

64. Jarvik, T., Smillie, C., Groisman, E. A. & Ochman, H. Short-term signatures of evolutionary change in the Salmonella enterica serovar typhimurium 14028 genome. *J Bacteriol* **192**, 560–567 (2010).

65. Datsenko, K. A. & Wanner, B. L. One-step inactivation of chromosomal genes in Escherichia coli K-12 using PCR products. *Proc Natl Acad Sci U S A* **97**, 6640–6645 (2000).

66. Figueroa-Bossi, N., Balbontín, R. & Bossi, L. Scarless DNA Recombineering. *Cold Spring Harb Protoc* **2023**, 638–650 (2023).

67. Schmieger, H. Phage P22-mutants with increased or decreased transduction abilities. *Mol Gen Genet* **119**, 75–88 (1972).

68. Balbontín, R., Vlamakis, H. & Kolter, R. Mutualistic interaction between Salmonella enterica and Aspergillus niger and its effects on Zea mays colonization. *Microb Biotechnol* **7**, 589–600 (2014).

69. Balbontín, R., Figueroa-Bossi, N. & Bossi, L. Construction of Single-Copy Fluorescent Protein Fusions by One-Step Recombineering. *Cold Spring Harb Protoc* **2023**, 651–662 (2023).

70. Maloy, S. R. & Roth, J. R. Regulation of proline utilization in Salmonella typhimurium: characterization of put::Mu d(Ap, lac) operon fusions. *J Bacteriol* **154**, 561–568 (1983).

445

450

TABLES AND FIGURES

Table 1. List of genes in the set of luciferase reporter fusions

Gene	Location	Function
iagB	SPI-1	SPI-1 type III secretion system invasion protein
pipB2	Orphan	SPI-1 effector
sseK3	ST64B	SPI-2 effector
sseC	SPI-2	SPI-2 effector
ssaV	SPI-2	SPI-2 effector
spvB	pSLT	Effector (TTSS-independent)
kdpD	Orphan	Two-component system, sensor histidine kinase
rfaB	Orphan	Galactosyltransferase
proV	Orphan	ATP-binding protein of glycine betaine/L-proline ABC transporter
nixA	Orphan	Putative nickel/cobalt transporter
entF	Orphan	Enterobactin synthetase
hupA	Orphan	HU nucleoid-associated protein
lsrF	Orphan	Quorum Sensing, autoinducer 2 aldolase
luxS	Orphan	Quorum sensing, autoinducer 2 synthase
rhs	SPI-6	Type VI secretion system

455

460

465

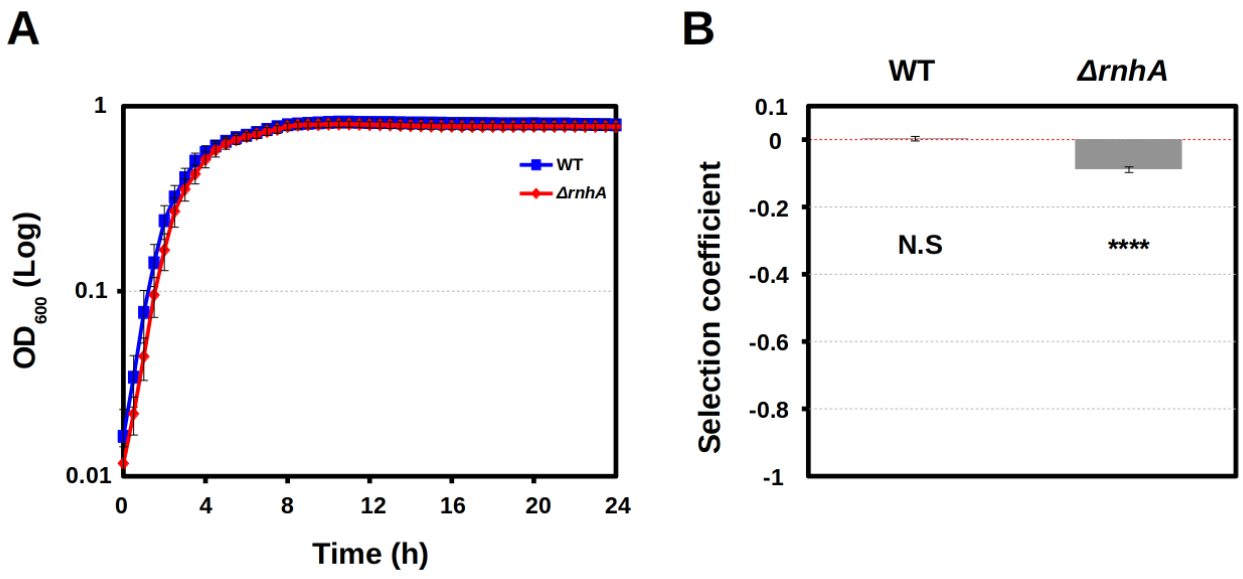

Figure 1. Fitness of the *ΔrnhA* mutant compared to wild-type bacteria. A. Growth curves of wild-type (blue dots and line) and *ΔrnhA* mutant (red dots and line) bacteria in LB. Dots represent the average and error bars represent standard deviation (n ≥ 47 independent biological replicates). **B.** Competitive fitness of wild-type and *ΔrnhA* mutant bacteria against a labeled wild-type reference strain in LB. Bars represent average and error bars standard deviation (n ≥ 3 independent biological replicates). N.S. non-significant; *P < 0.05; **P < 0.01; ***P < 0.001; ****P < 0.0001 (one-sample two-tailed Student's t test).

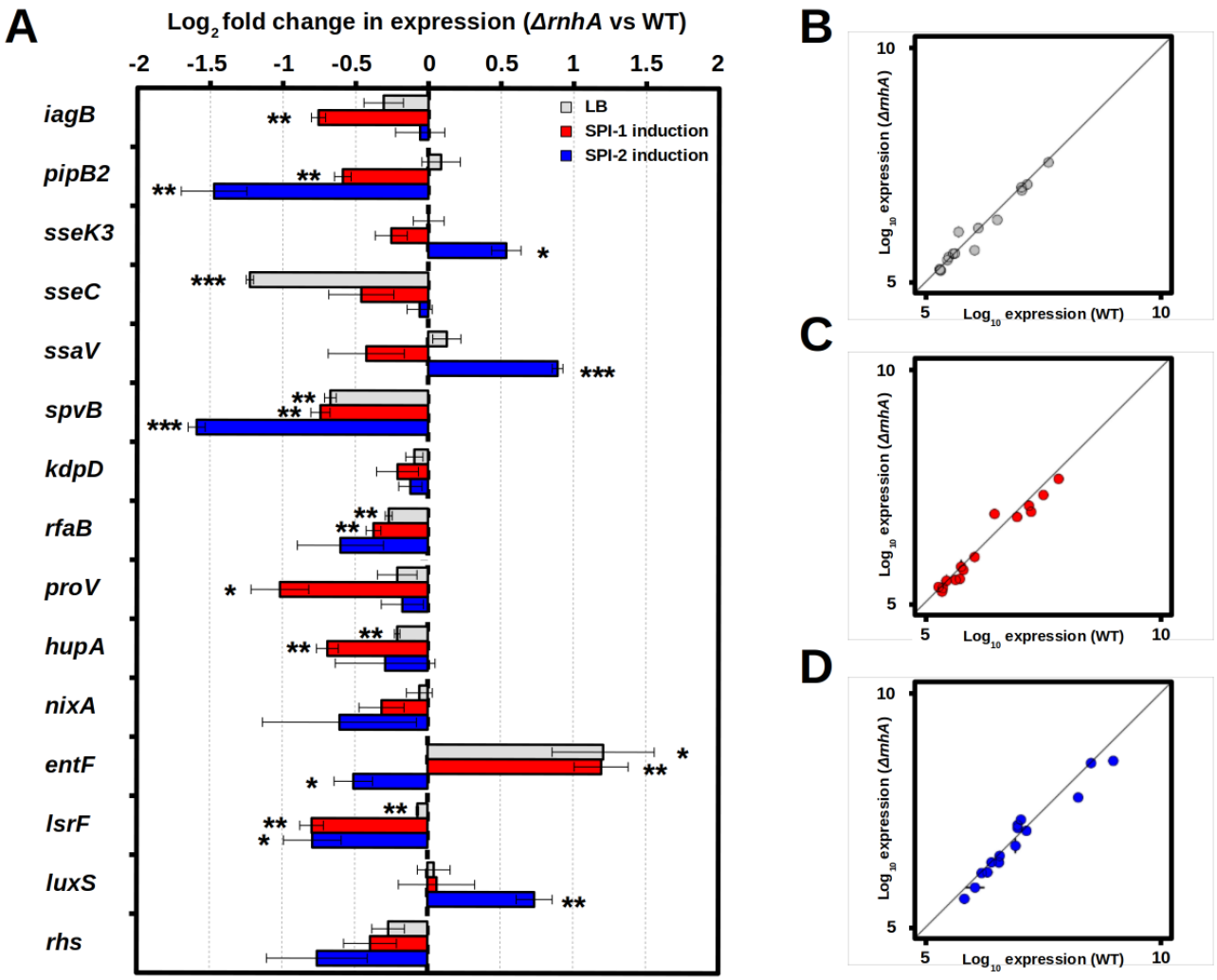

Figure 2. Expression of luciferase reporter fusions to genes associated with *S. enterica* virulence. **A.** Ratio *ΔrnhA*/WT of the area under the curve of luminiscence normalized to OD_{600} of different reporter fusions in LB (grey bars), LB 0.3M NaCl (red bars) or LPM (blue bars). Bars represent average and error bars standard deviation (n = 3 independent biological replicates). N.S. non-significant; *P < 0.05; **P < 0.01; ***P < 0.001; ****P < 0.0001 (one-sample two-tailed Student's t test). **B-D.** Logarithmic representation of the expression of luciferase reporter fusions in the WT (X axis) and the *ΔrnhA* (Y axis) backgrounds, either in LB (**B**), LB 0.3M NaCl (**C**) or LPM (**D**). The black diagonal line represents the linear regression if the expressions were identical.

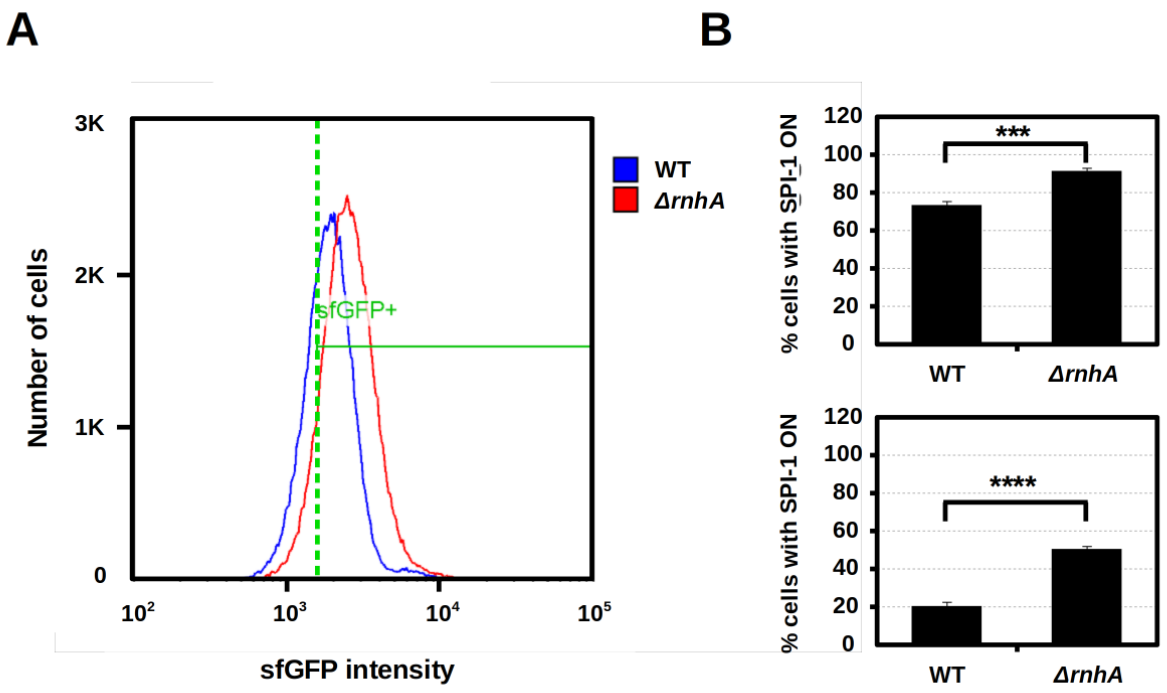

Figure 3. Lack of RNase HI affects fluorescence intensity of bacteria carrying the P_{sicA}-*sfGFP* fusion. A. Distribution of sfGFP fluorescence intensity in wild-type (blue line) and *ΔrnhA* (red line) bacteria carrying the P_{sicA}-*sfGFP* fusion, in LB. The vertical green dashed line represents the threshold of fluorescent versus non-fluorescent bacteria, determined using non-fluorescent bacteria as control. B. Percentage of cells with the P_{sicA}-*sfGFP* fusion in ON in wild-type and *ΔrnhA* bacteria, either in LB (top panel) or in NCE (bottom panel) media. Bars represent average and error bars standard deviation (n = 3 independent biological replicates). N.S. non-significant; *P < 0.05; **P < 0.01; ***P < 0.001; ****P < 0.0001 (two-tailed Student's t test).

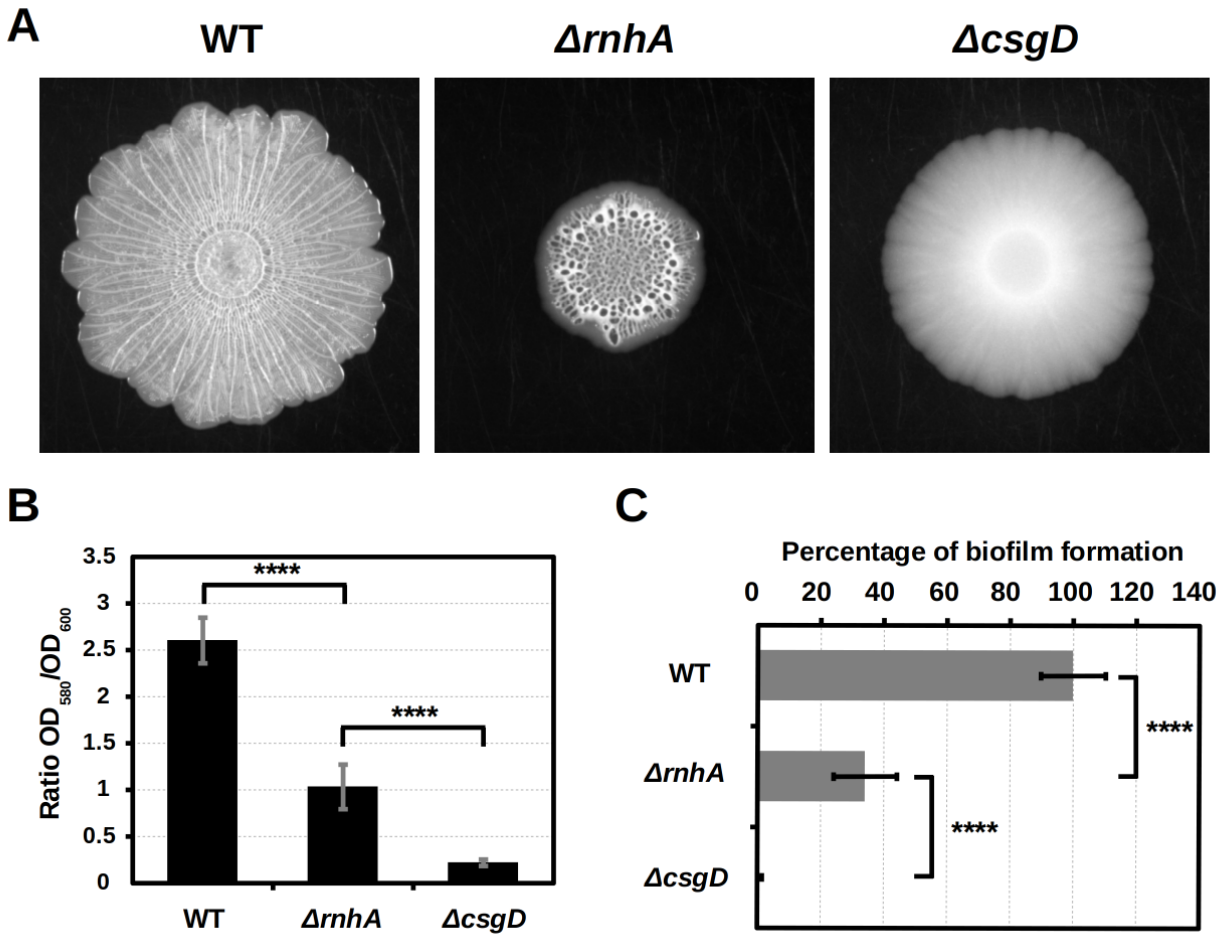

Figure 4. Lack of RNase HI causes reduction in biofilm formation. A. Colony morphology of wild-type bacteria (left panel), the *ΔrnhA* mutant (center panel) and the *ΔcsgD* mutant, unable to form biofilms (right panel), after 7 days of incubation at 30 ºC in LB agar without salt. **B.** Ratio between the OD_{580} (measuring concentration of crystal violet) and OD600 (measuring cell density) of wild-type bacteria, the *ΔrnhA* mutant and the *ΔcsgD* mutant, unable to form biofilms, after 48 h of incubation at 25 ºC in LB without salt. **C.** Percentage of biofilm formation of the *ΔrnhA* mutant with respect to wild-type bacteria (considered to form 100%) and the *ΔcsgD* mutant (considered to form 0%). Bars represent average and error bars standard deviation (n = 9 independent biological replicates). N.S. non-significant; *P < 0.05; **P < 0.01; ***P < 0.001; ****P < 0.0001 (two-tailed Student's t test).

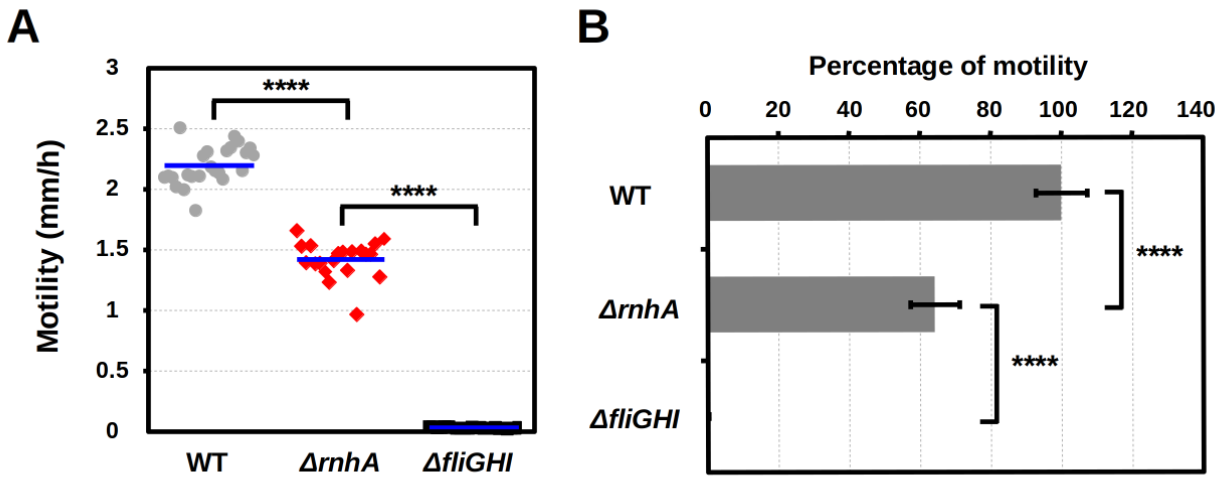

Figure 5. RNase HI depletion negatively affects bacterial motility. A. Motility (expressed in milimeters per hour) of wild-type bacteria, the *ΔrnhA* mutant, and the non-motile *ΔfliGHI* mutant. **B.** Percentage ofmotility of the *ΔrnhA* mutant with respect to wild-type bacteria (considered to move 100%) and the *ΔfliGHI* mutant (considered to move 0%). Bars represent average and error bars standard deviation (n ≥ 20 independent biological replicates). N.S. non-significant; *P < 0.05; **P < 0.01; ***P < 0.001; ****P < 0.0001 (two-tailed Student's t test).

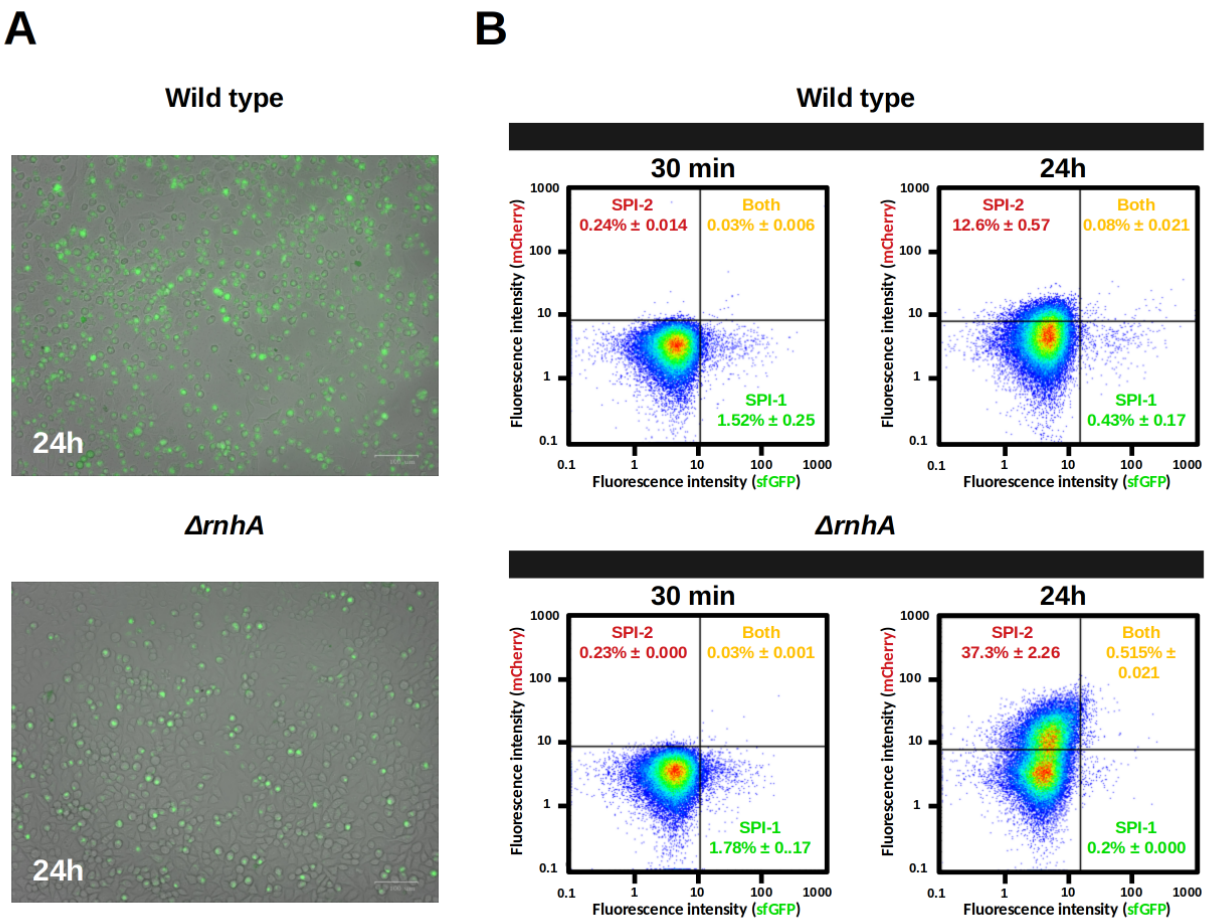

Figure 6. Lack of RNase HI affects expression of a P_{ssaB}-*mCherry* fusion during infection of epithelial cells. A. Fluorescence microscopy image of HeLa cells infected with wild-type (top panel) or *ΔrnhA* (bottom panel) bacteria constitutively expressing sfGFP at 24 h after infection. B. Distribution of sfGFP and mCherry fluorescence intensity in wild-type (top panel) and *ΔrnhA* (bottom panel) bacteria carrying the P_{ssaB}-*mCherry* fusion, within HeLa epithelial cells at 30 minutes and 24 h after infection. Thresholds for sfGFP and mCherry fluorescences were determined using strains expressing either fluorescence constitutively and non-fluorescent control strains.

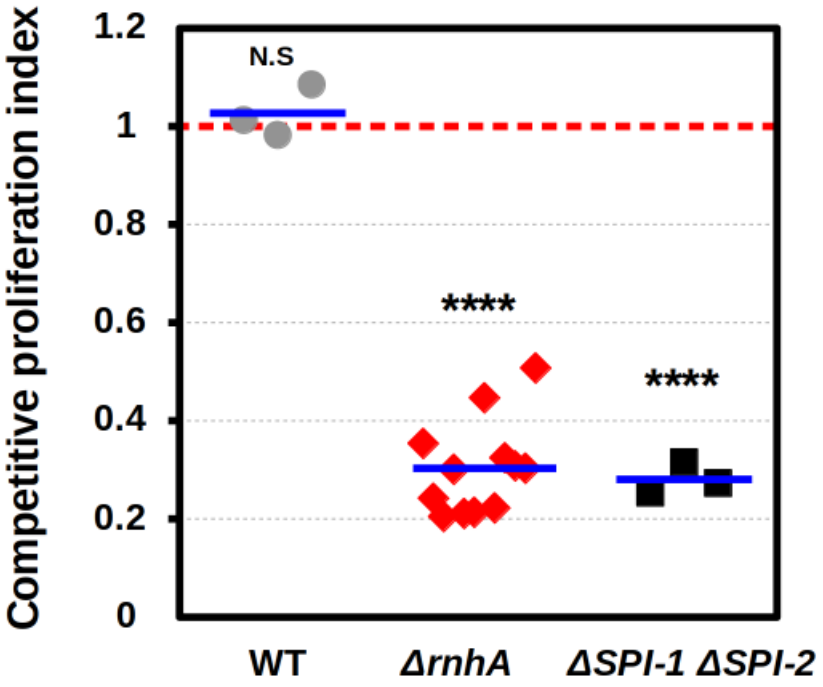

Figure 7. Mutants lacking RNase HI are defective in proliferation within macrophages. Competitive index in proliferation within murine macrophages of either wild-type bacteria (grey circles), a mutant lacking the two major *Salmonella* Pathogenicity Islands SPI-1 and SPI-2 (black squares), as negative control, and the *ΔrnhA* mutant (red diamonds). Horizontal bars represent the mean ($n \geq 3$ independent biological replicates). N.S. non-significant; * = $P < 0.05$; ** = $P < 0.01$; *** = $P < 0.001$;**** = $P < 0.0001$ (one-sample two-tailed Student's t-test).

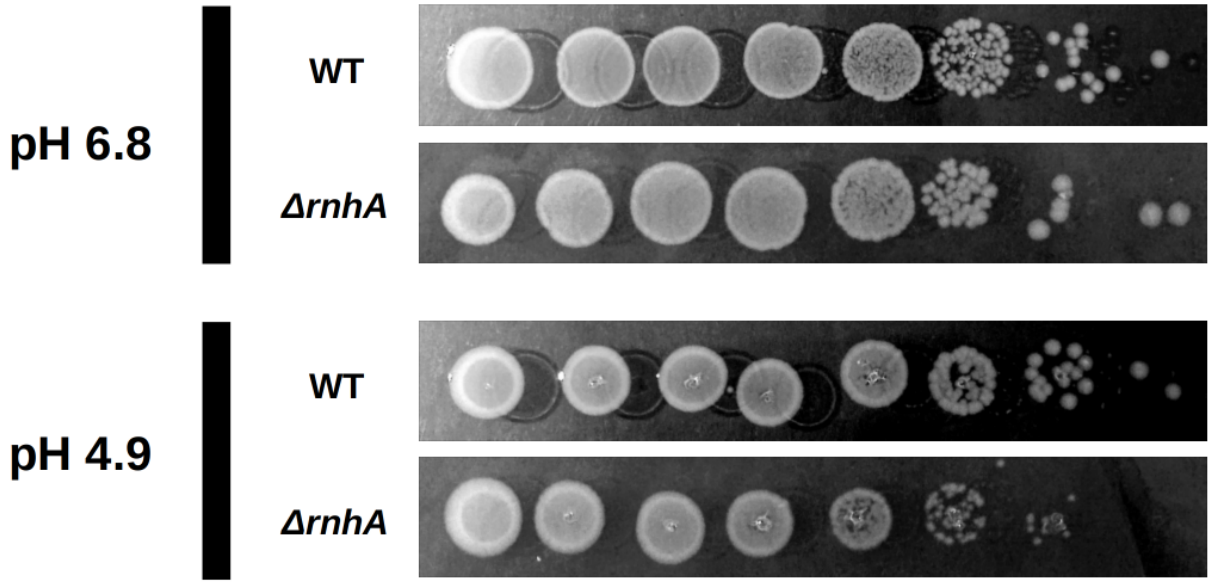

Figure S1. Lack of RNase HI increases sensitivity to low pH. Viability of serially diluted wild-type (top lanes) and *ΔrnhA* (bottom lanes) in LB at pH 6.8 (top panel) or 4.9 (bottom panel). The experiment included four biological replicates and four technical replicates; representative data sets are shown.

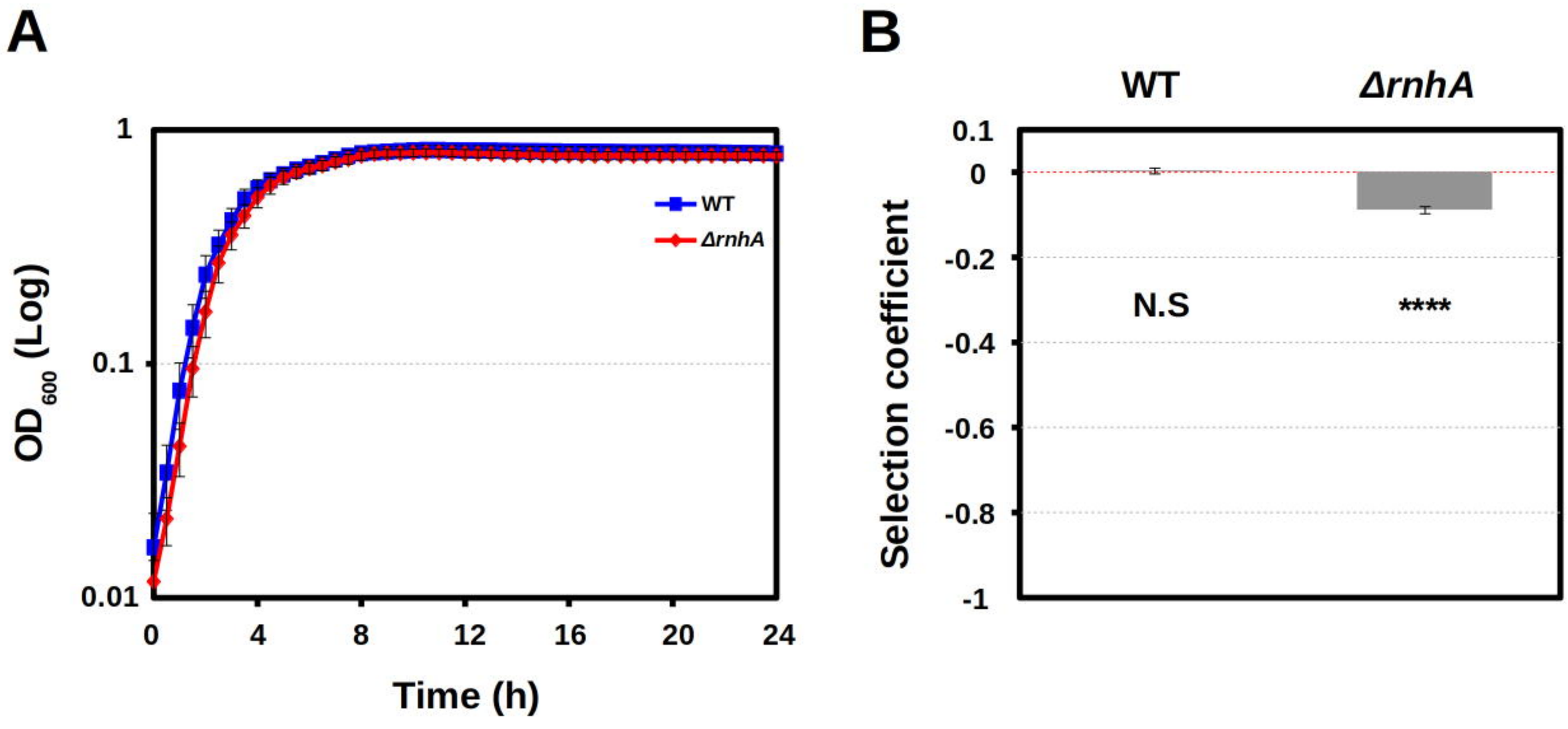
A
1
0.1
0.01
OD600 (Log)
0
4
8
12
16
20
24
Time (h)
WT
ΔrnhA
B
WT
ΔrnhA
0.1
0
-0.2
-0.4
-0.6
-0.8
-1
Selection coefficient
N.S
****

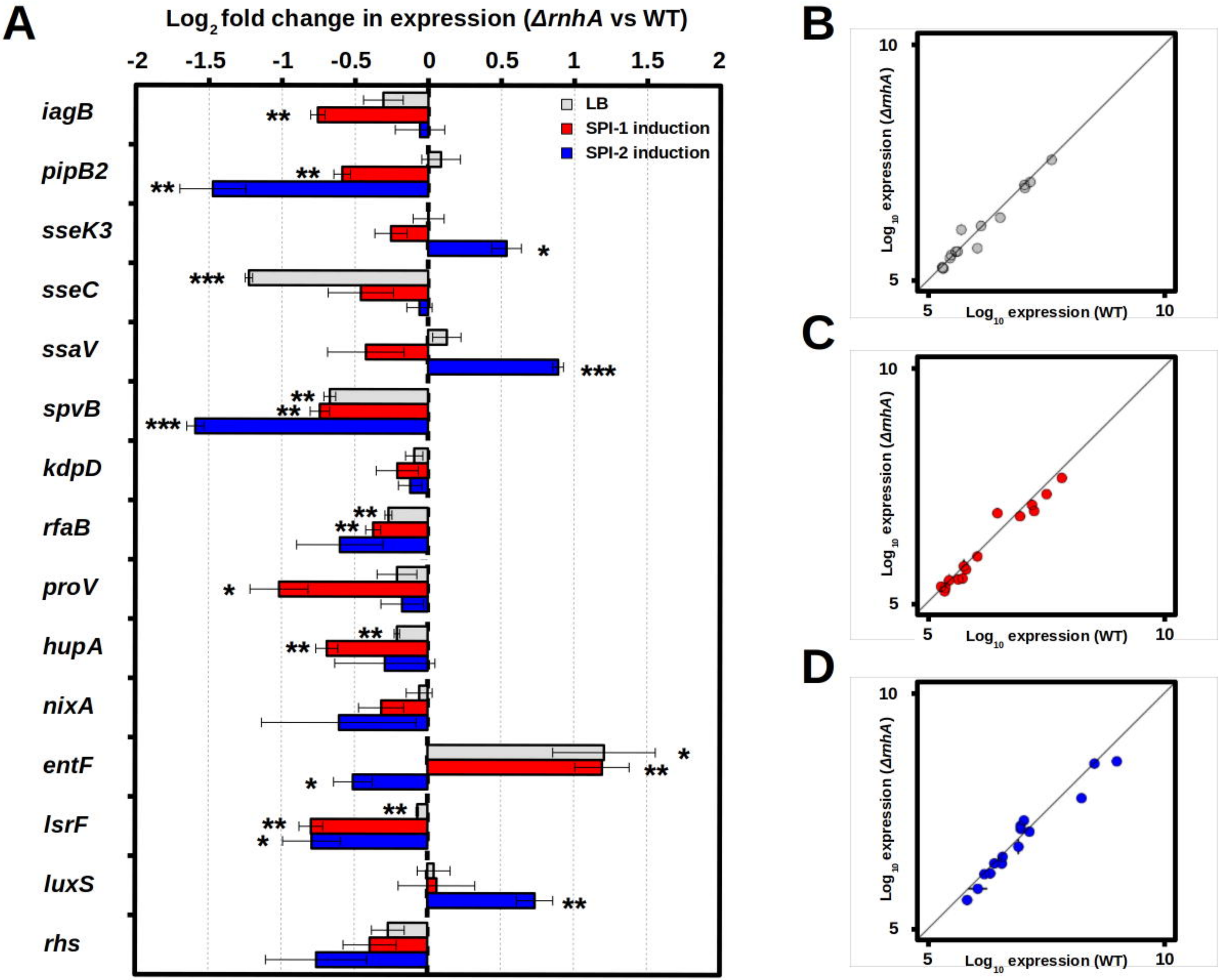
A
Log2 fold change in expression (ΔrnhA vs WT)
-2
-1.5
-1
-0.5
0
0.5
1
1.5
2
LB
SPI-1 induction
SPI-2 induction
iagB
pipB2
sseK3
sseC
ssaV
spvB
kdpD
rfaB
proV
hupA
nixA
entF
lsrF
luxS
rhs
B
Log10 expression (ΔmhA)
Log10 expression (WT)
C
Log10 expression (ΔmhA)
Log10 expression (WT)
D
Log10 expression (ΔmhA)
Log10 expression (WT)

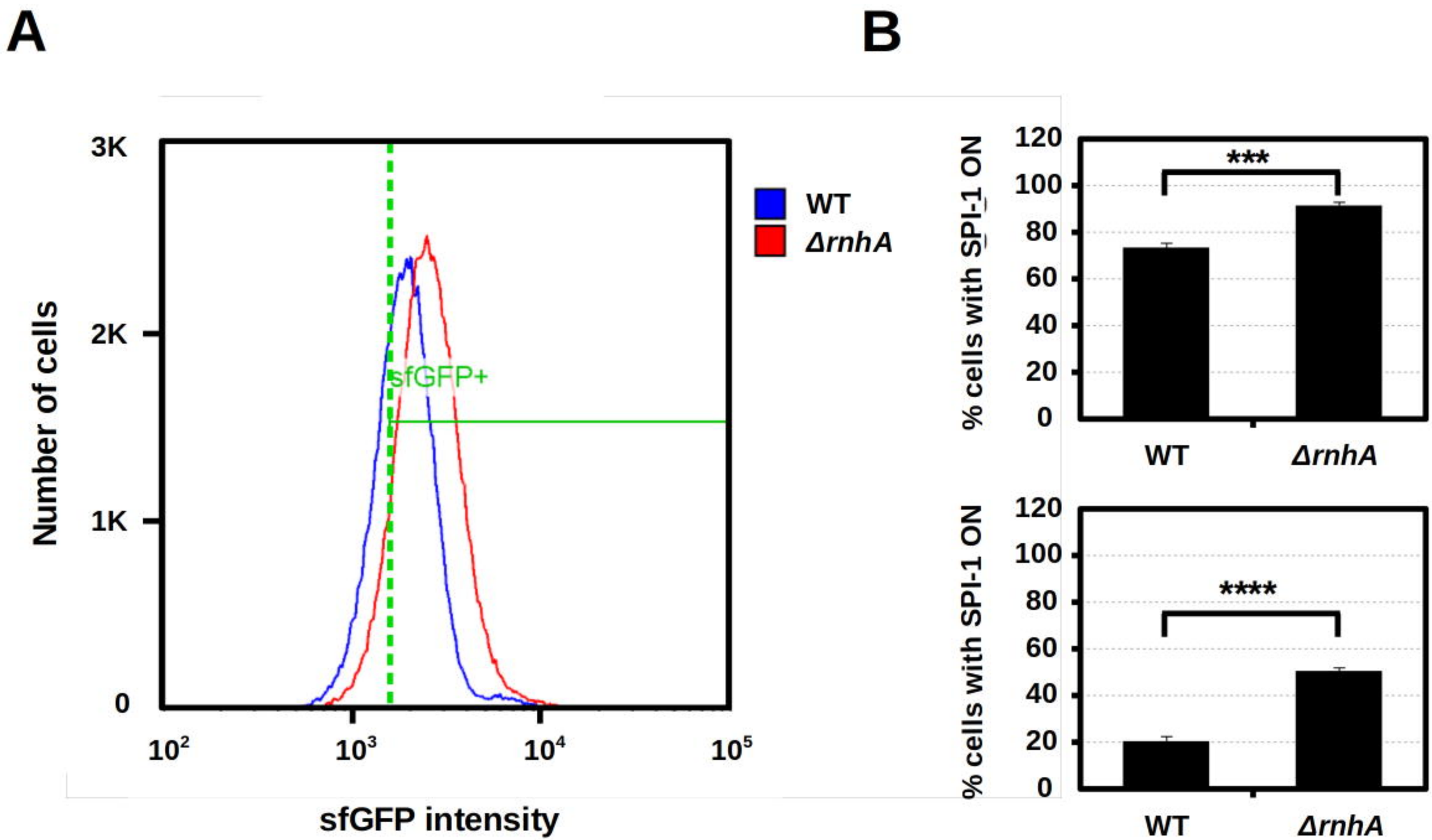
A
B
3K
2K
1K
0
Number of cells
sfGFP+
WT
ΔrnhA
10^2
10^3
10^4
10^5
sfGFP intensity
% cells with SPI-1 ON
120
100
80
60
40
20
0
***
WT
ΔrnhA
% cells with SPI-1 ON
120
100
80
60
40
20
0
****
WT
ΔrnhA

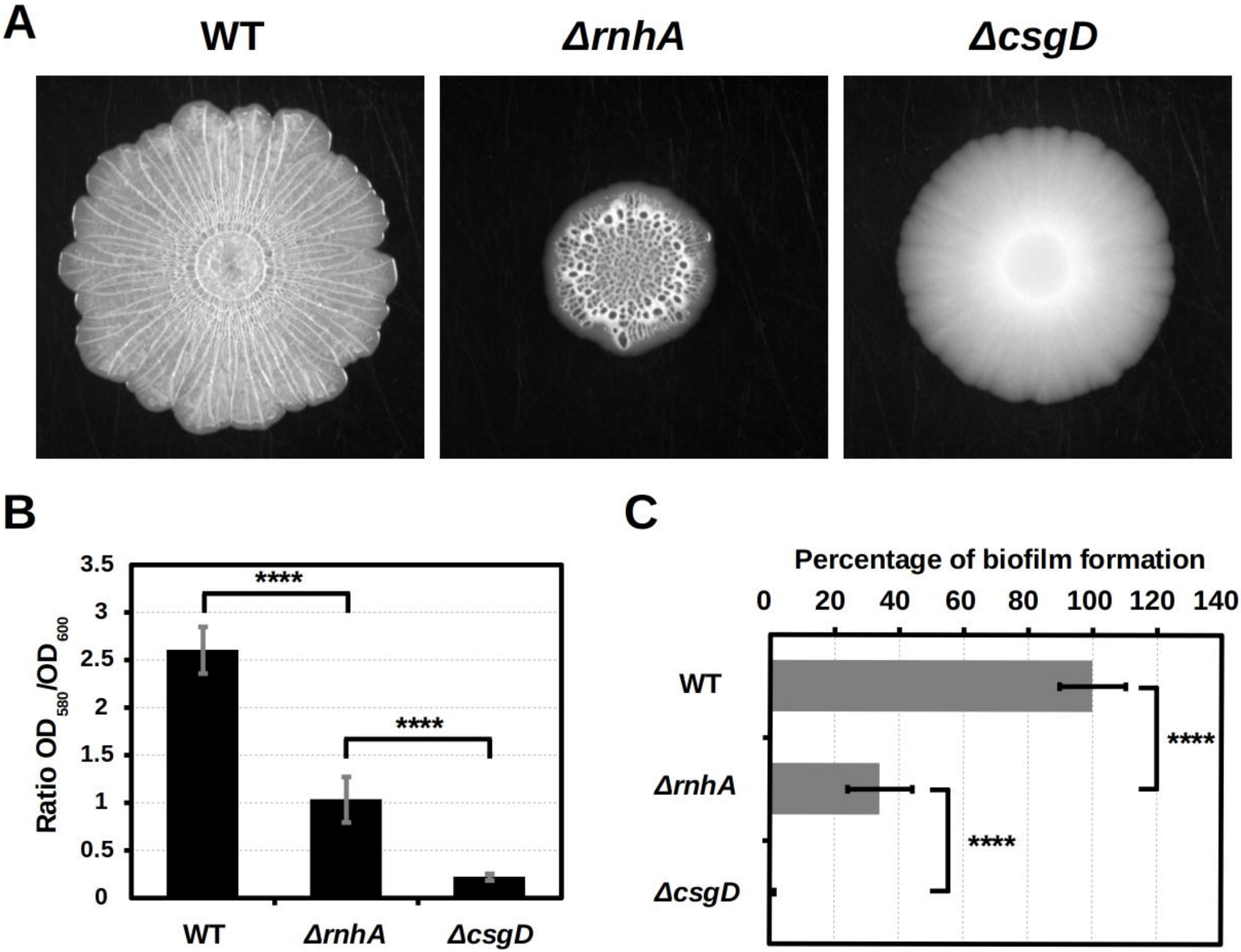
A
WT
ΔrnhA
ΔcsgD
B
Ratio OD580/OD600
3.5
3
2.5
2
1.5
1
0.5
0
****
****
WT
ΔrnhA
ΔcsgD
C
Percentage of biofilm formation
0
20
40
60
80
100
120
140
WT
ΔrnhA
ΔcsgD
****
****

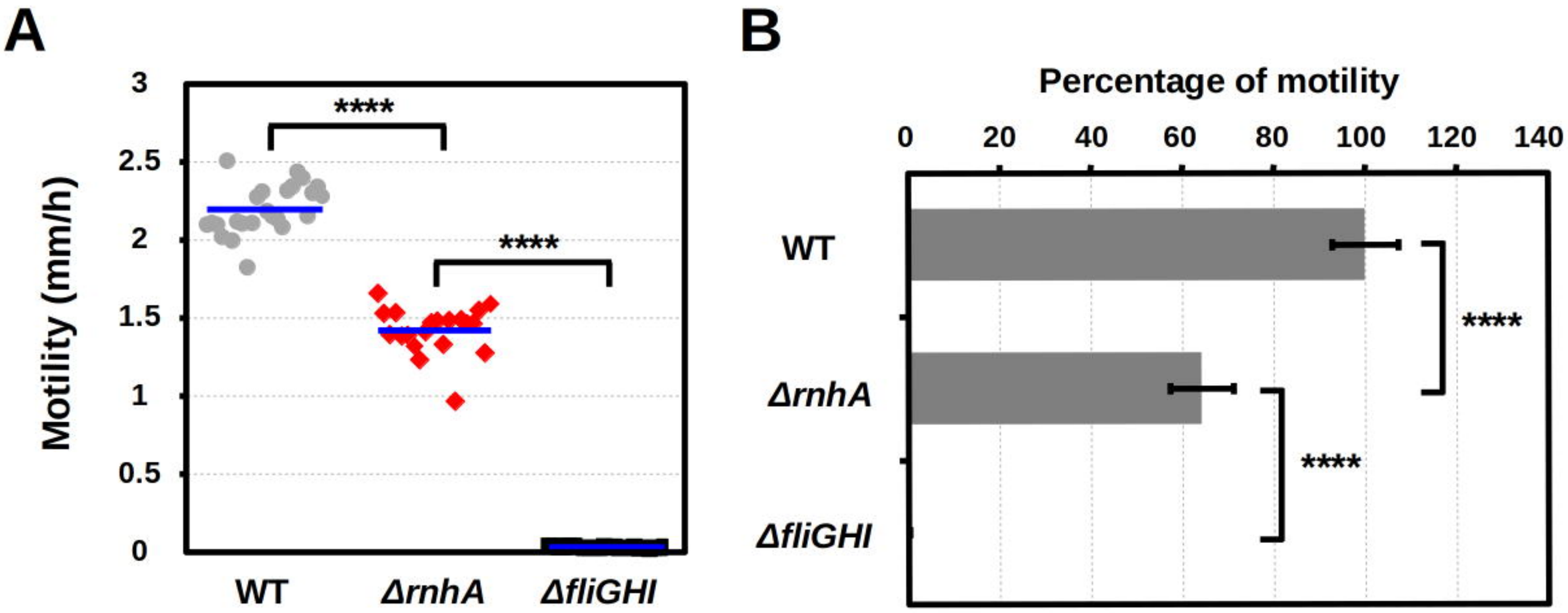
A
Motility (mm/h)
3
2.5
2
1.5
1
0.5
0
****
****
WT
ΔrnhA
ΔfliGHI
B
Percentage of motility
0
20
40
60
80
100
120
140
WT
ΔrnhA
ΔfliGHI
****
****

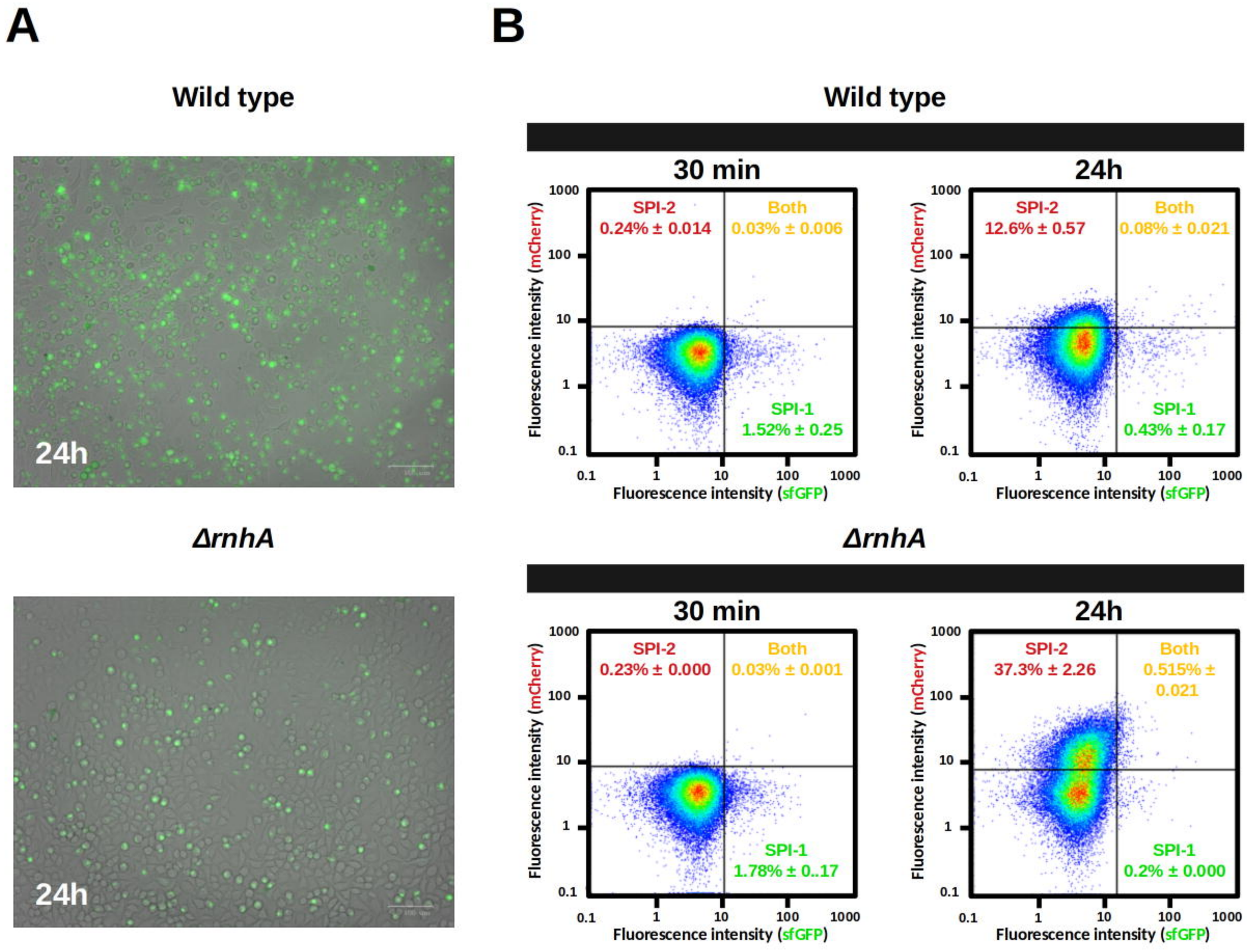
A
Wild type
24h
ΔrnhA
24h
B
Wild type
30 min
SPI-2
0.24% ± 0.014
Both
0.03% ± 0.006
SPI-1
1.52% ± 0.25
24h
SPI-2
12.6% ± 0.57
Both
0.08% ± 0.021
SPI-1
0.43% ± 0.17
ΔrnhA
30 min
SPI-2
0.23% ± 0.000
Both
0.03% ± 0.001
SPI-1
1.78% ± 0..17
24h
SPI-2
37.3% ± 2.26
Both
0.515% ± 0.021
SPI-1
0.2% ± 0.000
Fluorescence intensity (mCherry)
Fluorescence intensity (sfGFP)
0.1
1
10
100
1000

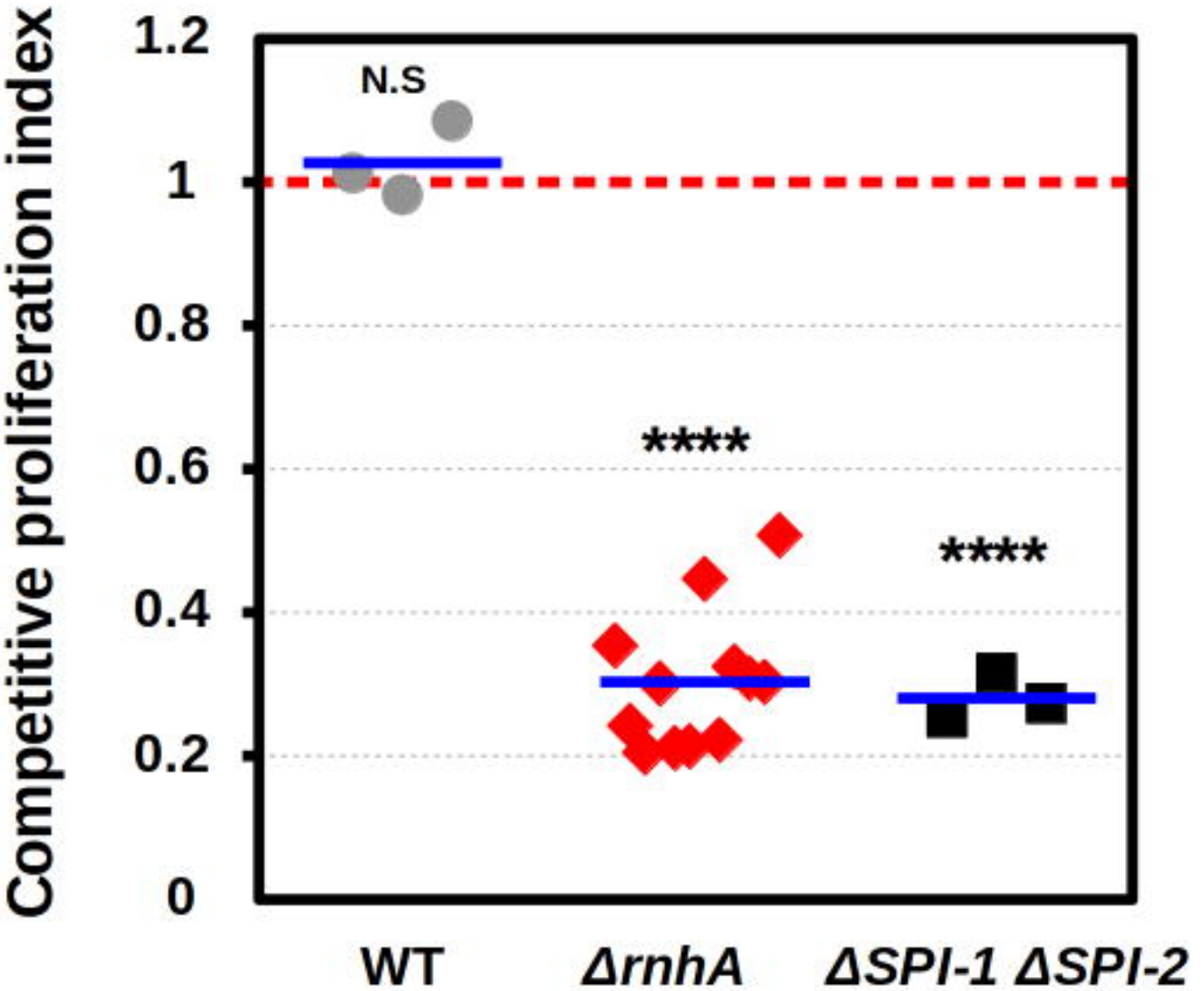
Competitive proliferation index
1.2
1
0.8
0.6
0.4
0.2
0
N.S
****
****
WT
ΔrnhA
ΔSPI-1 ΔSPI-2

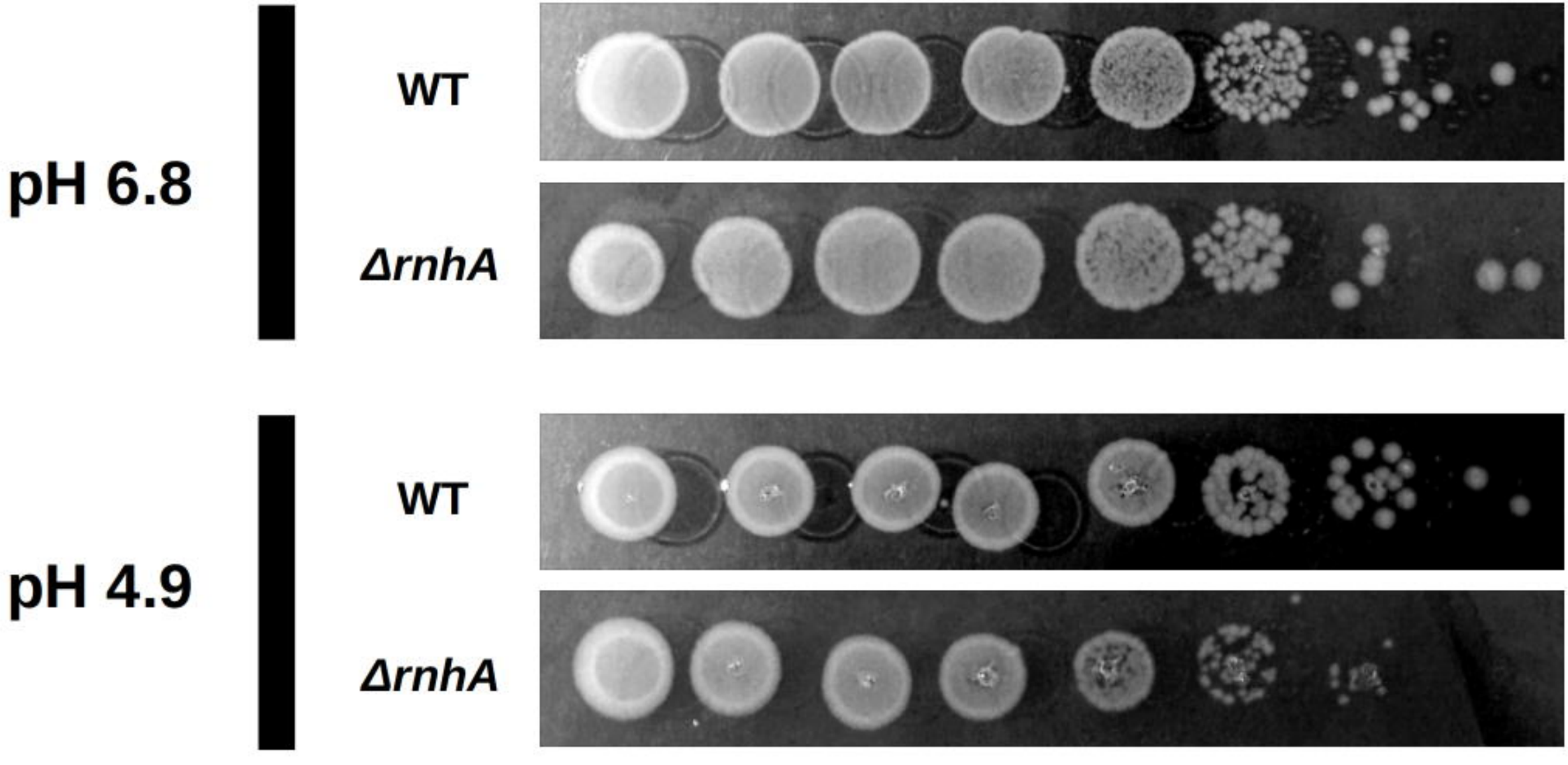
pH 6.8
WT
ΔrnhA
pH 4.9
WT
ΔrnhA